Radiative transfer code SHARM for atmospheric and terrestrial applications

A. I. Lyapustin

An overview of the publicly available radiative transfer Spherical Harmonics code (SHARM) is presented. SHARM is a rigorous code, as accurate as the Discrete Ordinate Radiative Transfer (DISORT) code, yet faster. It performs simultaneous calculations for different solar zenith angles, view zenith angles, and view azimuths and allows the user to make multiwavelength calculations in one run. The Delta-M method is implemented for calculations with highly anisotropic phase functions. Rayleigh scattering is automatically included as a function of wavelength, surface elevation, and the selected vertical profile of one of the standard atmospheric models. The current version of the SHARM code does not explicitly include atmospheric gaseous absorption, which should be provided by the user. The SHARM code has several built-in models of the bidirectional reflectance of land and wind-ruffled water surfaces that are most widely used in research and satellite data processing. A modification of the SHARM code with the built-in Mie algorithm designed for calculations with spherical aerosols is also described.

OCIS codes: 010.0010, 280.1310, 010.1300.

1. Introduction

In the past several years we have witnessed a dramatic expansion of knowledge about our environment that comes from operational ground-based and spaceborne remote-sensing systems. For example, the Moderate Resolution Imaging Spectroradiometer[1,2] (MODIS) and the Multiangle Imaging Spectroradiometer[3] (MISR) are instruments of a new generation that conduct global operational monitoring of a large number of atmospheric and surface parameters from space. The ground-based Aerosol Robotic Network[4] (AERONET) provides characterization of atmospheric column aerosol and water vapor for more than 170 locations worldwide. These and other sources of information dramatically enhance our capability to accurately model solar radiative transfer in the Earth–atmosphere system and improve our understanding of the radiative budget and climate forcing factors of our planet. Such research needs rigorous, fast, and user-friendly radiative transfer (RT) codes that can be directly used with the aerosol and surface reflectance models and data types available from the operational networks and spaceborne global observing systems.

There are several publicly available RT codes[5–10] for the atmospheric and land remote-sensing communities; the most broadly used are the one-dimensional codes Discrete Ordinate Radiative Transfer[5] (DISORT), Second Simulation of the Satellite Signal in the Solar Spectrum[6] 6S, and a three-dimensional code Spherical Harmonic Discrete Ordinate Method[7] (SHDOM). In this paper the latest version of the Spherical Harmonics code[11,12] (SHARM) upgraded with the Delta-M[13] method, and a modification of this code with the MIE algorithm[14] (SHARM-Mie), which is particularly convenient for the multiple-wavelength calculations with spherical aerosols, are described.

2. Overview

The SHARM code solves the monochromatic unpolarized plane-parallel one-dimensional problem with a vertically nonuniform atmosphere and several broadly used models of the land–ocean surface bidirectional reflectance factor (BRF). It calculates radiance and fluxes at the interfaces of atmospheric layers in the shortwave spectral region. When the surface is Lambertian, the SHARM code also calculates the path radiance, upward atmospheric trans-

A. I. Lyapustin (alyapust@pop900.gsfc.nasa.gov) is with the University of Maryland Baltimore County Goddard Earth Science Technology Center, and NASA Goddard Space Flight Center, code 614.4, Greenbelt, Maryland 20771.

Received 16 June 2005; revised 4 August 2005; accepted 5 August 2005.

0003-6935/05/367764-09$15.00/0

mittance, and spherical albedo of the atmosphere. The SHARM performs simultaneous calculations for the specified solar zenith angles (SZAs), view zenith angles (VZAs), and view azimuths and allows the user to handle multiple wavelengths in one run. Molecular scattering is added automatically according to the wavelength, surface height above the sea level, and selected atmospheric profile. The molecular absorption, as well as the optical properties of aerosols or clouds for each atmospheric layer, should be provided by the user. Details of the Method of Spherical Harmonics (MSH) algorithm, along with the built-in models, are given in Appendix A.

The code comes in a package with the program PHASE, which computes Legendre expansion coefficients of aerosol or cloud phase function $\chi(\gamma)$, where γ is the angle of scattering, and automatically normalizes it. The rational spline interpolation is used to compute the phase function in the quadrature angles required for the Legendre expansion and in the directions required for the single-scattering calculations. The rational spline provides an accurate smooth interpolation for most anisotropic phase functions, for which the conventional cubic spline often develops an oscillating error. The current version of the PHASE program calculates as many as 2000 nonzero Legendre coefficients by using the high-order Lobatto quadrature.

The input data are arranged in three files, as follows: The Configuration file (config.par) defines wavelengths, the order of the MSH, the incidence-view geometry, and the file names of input atmospheric and surface properties and governs printing of the results.

The Atmospheric Properties file describes the model of the atmosphere and the optical properties of aerosols or clouds. In the SHARM code the input includes the optical thickness ($\Delta\tau$), the single-scattering albedo (ω), and the scattering function of aerosols or clouds for each atmospheric layer. The molecular absorption is not automatically included in this version and should be provided by the user.

The Surface Properties file describes the model and parameters of the surface reflectance. The details of the parameters and the input format are documented in the SHARM Manual.[15]

The other code, SHARM–Mie, is an integrated package that combines Mie calculations for the wavelengths of interest, automatic Legendre expansion of phase functions, and RT calculations with the SHARM code. Aerosols are represented by polydisperse spherical particles with the bimodal or a generic-form lognormal size distribution. The aerosol properties are assumed to be constant with altitude, but aerosol concentration may vary according to the specific vertical profile. This approach was chosen to reduce the overall computing time because the main computational load is carried by the Mie calculations. The resultant atmospheric model is quite realistic, however, and well suited for the remote-sensing studies of atmospheric aerosol and surface reflectance.

The monodisperse Mie calculations in the SHARM-Mie code are performed by Wiscombe's code MIEVnoP (Ref. 14) translated into C language. The integration over size distribution is carried out with Simpson's quadrature with 2001 points. The integration limits are either given by the minimum and maximum radii of the generic-form size distribution or set to $r_{\min} = 0.05$ μm and $r_{\max} = 15$ μm for the bimodal distribution. For the Legendre expansion, the phase function is directly computed in the Lobatto qudrature points with subsequent integration with the Legendre polynomials. This algorithm is faster[14] than the MIEV code, which calculates Legendre coefficients for the monodisperse aerosol.

The input for the SHARM-Mie code differs from that of SHARM code in the Atmospheric Properties file. Instead of optical parameters $\{\Delta\tau,\ \omega,\ \chi(\gamma)\}$, the user should specify the relative vertical profile of aerosol and its microphysical properties, namely, spectral index of refraction and particle size distribution.

The SHARM and SHARM-Mie codes share a common library of files and are written in C language with C++ features.

3. Built-In Models

A. Geometric Model

The SHARM uses a plane-parallel model of the atmosphere divided into K homogeneous layers. Each layer k is characterized by its optical thickness $\Delta\tau_k = \tau_k - \tau_{k-1}$, single-scattering albedo ω_k, and scattering function $\chi_k(\gamma)$. The total optical thickness and atmospheric layers are counted from the top of the atmosphere. By contrast, the altitude of the interfaces (h_i) is counted from the ground level, in agreement with the standard atmospheric profiles of temperature and pressure.

In the accepted coordinate system, SZA θ_0 changes from 0 to 90° and VZA θ changes in the ranges 90°–180° ($\mu = \cos\theta < 0$) for upward directions (view geometry from space) and 0°–90° ($\mu > 0$) for downward directions (ground-based observations of sky radiance). The relative azimuth is calculated clockwise from the principal plane: it is defined such that $\varphi = 0°$ for the forward scattering and $\varphi = 180°$ for the backscattering directions.

B. Rayleigh Scattering

The scattering function of air is considered to be purely Rayleigh; it does not account for a slight asymmetry caused by depolarization. The vertical profile of molecular optical thickness is calculated as

$$\tau^m(\lambda, z) = \int_0^z \sigma(\lambda, z')N(z')\mathrm{d}z',$$

where σ is a Rayleigh scattering cross section per molecule,

$$N(z) = N_s \frac{P(z)}{P_s} \frac{T_s}{T(z)}$$

is the concentration of air molecules at altitude z, and $P_s = 1013.25$ mb, and $T_s = 273.15$ K are the standard pressure and temperature, respectively. The vertical profile of pressure and temperature can be selected from six standard atmospheric profiles[16] (Tropical, Midlatitude Summer, Midlatitude Winter, Subarctic Summer, Subarctic Winter, and 1976 U.S. Standard). The integral over altitude is evaluated with the Gaussian quadrature.

The Rayleigh scattering cross section is calculated with the algorithm of Bodhaine *et al.*,[17] which has a uniformly high accuracy across the spectral range from UV to the shortwave IR.

C. Surface BRF Models

Three broadly recognized BRF models of land-surface reflectance are built in both the SHARM and the SHARM-Mie codes: the Rahman–Pinty–Verstraete[18] (RPV) model, the modified RPV[19] (MRPV) model, and the Li Sparse–Ross Thick reciprocal[20] (LSRT) model. The LSRT and MRPV models are used in the operational land-reflectance algorithms of the MODIS and the MISR, respectively. All these models are reciprocal and rotationally invariant; i.e., they depend only on the relative azimuth and are described by three parameters.

The ocean surface reflectance can be modeled with either the azimuthally independent model of Nakajima and Tanaka[21] or the Cox–Munk[22] model with Gram–Charlier expansion. Both models include the bidirectional wave-shadowing factor of Nakajima and Tanaka.[21] The Nakajima–Tanaka model depends only on the wind speed, whereas the Grams–Charlier model additionally depends on the wind direction. The details of surface BRF models are given in Appendix A.2.

4. Accuracy, Convergence, and Speed of the SHARM Code

The SHARM Code was extensively compared[11,23] with the DISORT code and was also indirectly tested in the atmospheric correction of airborne measurements, e.g., over the dark ocean.[24]

The most important parameter that controls the accuracy of a solution is the order of the MSH (parameter nb) specified by the user. In essence, exactly nb coefficients of expansion of the phase function are used in the multiple-scattering calculations. The single-scattered radiance in the SHARM is calculated by use of an exact formula and does not depend on nb. The solution for the multiple scattering converges to the true solution at the increase of nb; however, the computing time also grows approximately as nb.[3]

Generally, the more asymmetric the phase function, the higher nb required for achieving a given accuracy. For typical continental or marine aerosols, a relative accuracy of 0.2–0.3% is achieved at $nb = 24$–36 in radiance calculations for VZAs and SZAs as high as 75°–80°. The value of $nb = 128$ ensures an accuracy of $\approx$0.02%.[23] Generally, the convergence slows with increasing zenith angle. Therefore, higher orders nb should be used for high SZAs or VZAs to achieve the same relative accuracy.

For calculations with the strongly asymmetric phase functions that are typical of clouds with large forward-scattering peaks, even high orders of MSH may be insufficient. For these cases we implemented the Delta-M method[13] that achieves accuracy within 1% at relatively low orders of MSH, $nb = 32$–64, except in the aureole region and some transitional area about it (see also the study in Ref. 25). As an example, Fig. 1 shows the convergence of the SHARM with and without the Delta-M method for cirrus cloud over an anisotropic surface.

The above discussion of accuracy and convergence pertains to radiance calculations (specific intensity). Flux calculations require considerably smaller orders of MSH. For example, fluxes at $nb = 12$–24 are typically accurate to the fourth significant digit.

The performance of the SHARM code was tested against that of the DISORT code[11,23] and the 6S code.[23] In single-angle calculations over a Lambertian surface, the speed of the SHARM was found to be a factor of 1.5–6 higher than that of the DISORT, depending on the number of atmospheric layers and on the selected order of solution (with $nb = N_{\text{streams}}$). This difference additionally increases several times when the surface reflects anisotropically.[23] Because the SHARM solves the RT problem for all incidence-view angles simultaneously, it offers a particular advantage in calculations with complex geometries. By comparison, the DISORT requires a separate solution for each SZA, whereas code 6S handles only one incidence and one view angle at a time. A detailed performance comparison among the codes SHARM, DISORT, and 6S is given in Table 1 of Ref. 23.

At typical orders of MSH ($nb = 24$–48), the run time of the code SHARM–Mie is almost entirely defined by Mie calculations. To minimize the run time, only nb required coefficients of Legendre expansion are calculated each time.

5. Conclusions

In this paper we have presented an overview of the code SHARM (SHARM–Mie), which is a rigorous yet fast code compared with similar codes. The SHARM offers a certain level of user convenience, such as built-in models of Rayleigh scattering and land–water surface reflectance, capability to perform simultaneous calculations for all specified geometries, and handling of multiple wavelengths in one run. The code is designed for a broad range of applications. It is particularly convenient for research in aerosol and land surface remote sensing and for generation of the massive lookup tables required by retrieval algorithms.

The present version of the SHARM code does not explicitly include atmospheric gaseous absorption, which is an important feature of several integrated

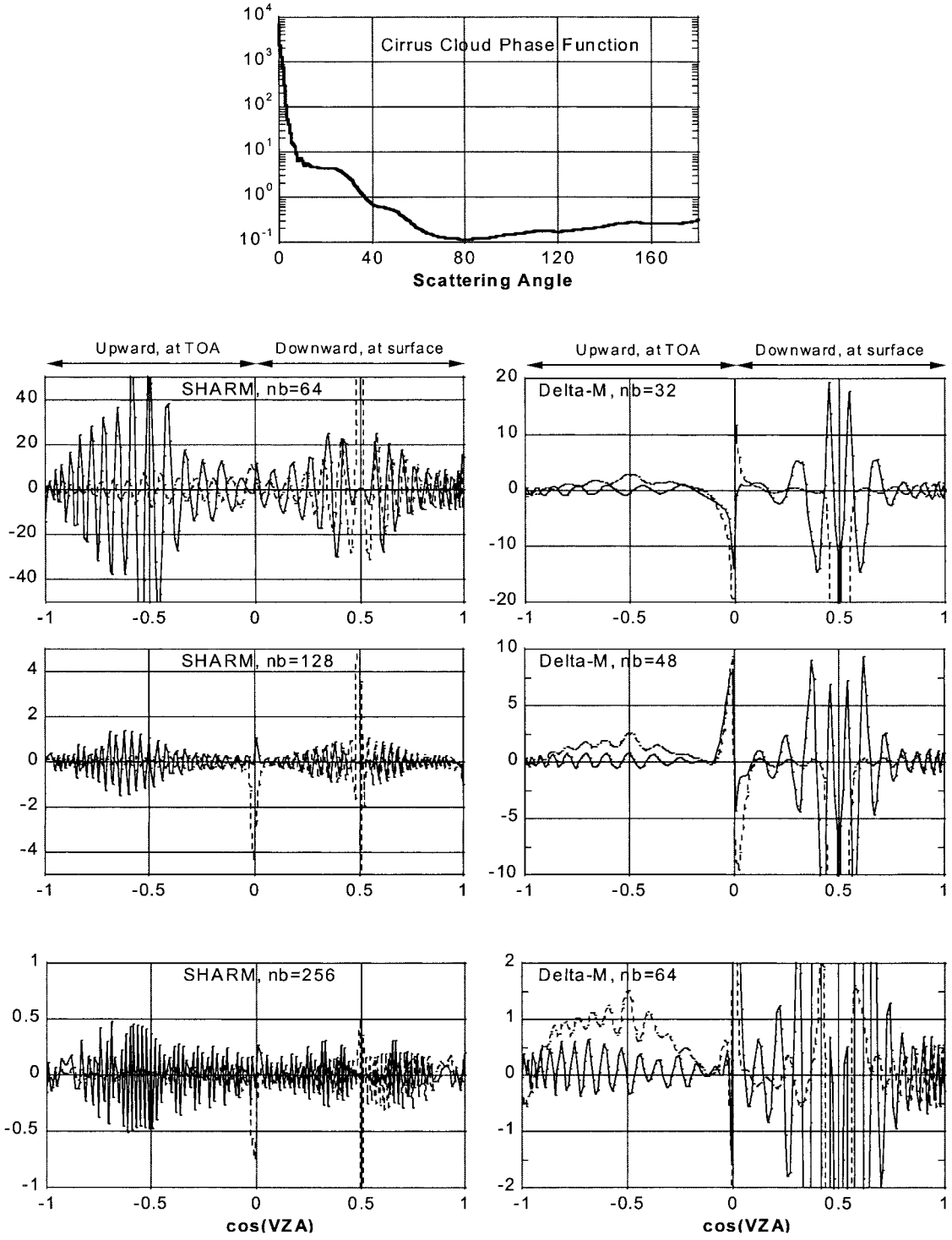

Fig. 1. Convergence of the SHARM code (left) and the SHARM with Delta-M code (right) for cirrus cloud. The results are shown as relative error (%) of SHARM radiance for different orders of MSH calculated with respect to the solution with $nb = 512$. Calculations were performed for $\tau = 0.8$ and a SZA of 60°. Solid and dashed curves represent relative azimuths of 0° and 180°, respectively. The negative and positive values on the abscissa axis relate to the upward radiance at the top of the atmosphere (TOA), and to the diffuse sky radiance incident upon surface, respectively. The cirrus cloud phase function at $\lambda = 0.66$ μm corresponds to ice particles with an effective diameter of 10 μm (http://www.ssec.wisc.edu/~baum/Cirrus/IceCloudModels.html).

RT packages.[8–10,15] Currently we are upgrading the SHARM code with the interpolation and profile correction method,[26] which will automatically model molecular absorption and will permit calculations with an arbitrary spectral resolution, from monochromatic to the shortwave broadband. Current versions of codes SHARM and SHARM–Mie can be downloaded from ftp://ltpftp.gsfc.nasa.gov/projects/asrvn/.

Appendix A

1. Method of Spherical Harmonics

Diffuse radiance $I(\tau;\ \mu,\ \varphi)$ is a solution to the following boundary-value problem:

$$\mu \frac{\partial I(\tau,\ \mu,\ \varphi)}{\partial \tau} + I(\tau,\ \mu,\ \varphi) = \frac{\omega}{4\pi} \int_0^{2\pi} d\varphi' \int_{-1}^{1} \times \chi(\tau,\ \gamma) I(\tau,\ \mu',\ \varphi') d\mu' + S_\lambda \frac{\omega}{4} \chi(\tau,\ \gamma_0) \times \exp\left(-\frac{\tau}{\mu_0}\right),$$

$$I(0;\ \mu,\ \varphi) = 0, \qquad \mu > 0, \tag{A1a}$$

$$I(\tau_0,\ \mu,\ \varphi) = S_\lambda \mu_0 \rho(\mu_0,\ \mu,\ \varphi - \varphi_0) \exp\left(-\frac{\tau_0}{\mu_0}\right) + \frac{1}{\pi} \int_0^{2\pi} d\varphi' \int_0^{1} \rho(\mu',\ \mu,\ \varphi - \varphi') \times I(\tau_0,\ \mu',\ \varphi') \mu' d\mu',\ \mu < 0. \tag{A1b}$$

Here ρ is a surface BRF (unitless) and πS_λ is extraterrestrial spectral solar irradiance. The scattering function is normalized to unity: $\frac{1}{2}\int_0^\pi \chi(\gamma)\sin\gamma d\gamma = 1$.

To solve problem (A1), the scattering function is expanded into Legendre polynomial series:

$$x(\gamma) = \sum_{n=0}^{L} \chi_n P_n(\cos\gamma),$$

with coefficients

$$\chi_k = \frac{2k+1}{2} \int_{-1}^{1} \chi(y) P_k(y) dy.$$

Parameter $L = nb$, the order of MSH, defines the accuracy of expansion and of the solution for multiple scattering.

The application of the addition theorem for Legendre polynomials and the expansion of radiance into spherical harmonics transforms integrodifferential equations (A1) into the system of linear differential equations:

$$A^m \frac{d\boldsymbol{\varphi}^m(\tau)}{d\tau} + C^m \boldsymbol{\varphi}^m(\tau) = \exp(-\tau/\mu_0)\mathbf{f}^m(\tau). \tag{A2}$$

Here $\boldsymbol{\varphi}^m(\tau) = \{\varphi_m{}^m(\tau),\ \varphi_{m+1}{}^m(\tau),\ \ldots,\ \varphi_{L_m}{}^m(\tau)\}^{\mathrm{T}}$ is the vector of moments for the mth azimuthal harmonic of radiance $I^m(\tau,\ \mu)$:

$$I(\tau;\ \mu,\ \varphi) = \sum_{m=0}^{\infty} (2 - \delta_{0,m}) I^m(\tau,\ \mu)\cos m\varphi,$$

$$I^m(\tau,\ \mu) = \sum_{k=m}^{L_m} \frac{2k+1}{2} \varphi_k{}^m(\tau) Y_k{}^m(\mu). \tag{A3}$$

In Eq. (A3),

$$Y_k{}^m(\mu) = \left[\frac{(k-m)!}{(k+m)!}\right]^{1/2} P_k{}^m(\mu)$$

are the normalized associated Legendre polynomials. Explicit expressions for matrices A^m and C^m and vector $\mathbf{f}^m$ can be found in Refs. 11 and 27. We use the triangular system of Eq. (A2), and the order of MSH $L_m - m + 1$ is even for all m.

The boundary conditions at the top and at the bottom of the atmosphere are expressed for the mth azimuthal harmonic in a form given by Marshak, as follows[12,28]:

$$\boldsymbol{\varphi}_{\mathrm{od}}{}^m(0) - G^m \boldsymbol{\varphi}_{\mathrm{ev}}{}^m(0) = 0, \tag{A4a}$$

$$(I - 2N_{\mathrm{od}}{}^m)\boldsymbol{\varphi}_{\mathrm{od}}{}^m(\tau_0) + (G^m - 2N_{\mathrm{ev}}{}^m)\boldsymbol{\varphi}_{\mathrm{ev}}{}^m(\tau_0) = 2S_0 \exp(-\tau_0/\mu_0)\mathbf{Q}^m(\mu_0), \tag{A4b}$$

where $\boldsymbol{\varphi}_{\mathrm{od}}{}^m$ and $\boldsymbol{\varphi}_{\mathrm{ev}}{}^m$ are vectors that consist of odd and even elements of vector $\boldsymbol{\varphi}^m$, respectively, and I is an identity matrix. Matrix G^m and a method for its calculation can be found in Ref. 28. $N_{\mathrm{od}}{}^m$ and $N_{\mathrm{ev}}{}^m$ are quadratic matrices of the order of $(L_m - m + 1)/2$:

$$(N_{\mathrm{ev}}{}^m)_{l,k} = (4k + 2m + 2\delta_m - 3) \times \int_0^1 \mu' Q_l{}^m(\mu') Y_{m+\delta_m+2k-2}{}^m(\mu') d\mu', \tag{A5a}$$

$$(N_{\mathrm{od}}{}^m)_{l,k} = (4k + 2m - 2\delta_m - 1) \times \int_0^1 \mu' Q_l{}^m(\mu') Y_{m-\delta_m+2k-1}{}^m(\mu') d\mu',$$

$$l,\ k = 1,\ 2,\ \ldots,\ \frac{L_m - m + 1}{2}, \tag{A5b}$$

where $\delta_m = 0$ if m is even and $\delta_m = 1$ if m is odd. The elements of vector $\mathbf{Q}^m(\mu')$ are calculated from azimuthal harmonics of the BRF:

$$Q_l{}^m(\mu') = \int_{-1}^{0} \rho^m(\mu',\ \mu) Y_{m-\delta_m+2l-1}{}^m(\mu) d\mu. \tag{A5c}$$

Previously, Lyapustin and Muldashev[12] used analytical formulas to integrate Eqs. (A5). Our further research with the BRF models built in the SHARM showed that the use of Gaussian quadrature permits faster integration with automatic selection of the quadrature order [$\approx(nb/2) + 10$].

A. Solution for Radiance

Solving the system of Eqs. (A2) and (A4) for each $m = 0,\ 1,\ \ldots$ for vectors $\varphi^m(\tau)$ allows the diffuse radi-

ance in the next step to be computed by summing Eqs. (A3). Harmonics $I^m(\tau, \mu)$ rapidly decrease in magnitude with increasing m, which terminates the azimuthal series at some M_0.

The method of solution is an analytical integration of Eq. (A2) within each atmospheric layer where atmospheric optical properties are constant (as well as matrices A^m and C^m and vector $\mathbf{f}^m$). After that, the singular-value decomposition of matrix $B^m = (C^m)^{-1} A^m$ rigorously transforms the resultant system of linear differential equations into the system of linear algebraic equations in K atmospheric layers with a block matrix,[27] which is successfully solved by a generalized Gauss elimination method.[11] Further, the solution is smoothed by the correction function method,[11] which compensates for errors that are due to truncation of the system of MSH and to an approximate form of the boundary conditions. This smoothing method also calculates the single-scattered radiance exactly, regardless of the order of approximation of the MSH.

If a surface is Lambertian, the SHARM code separately computes atmospheric path radiance D, which is a solution with a black surface, a surface irradiance $\pi E_0(\mu_0)$, upward atmospheric transmittance $T(\mu)$, and the spherical albedo of atmosphere c_0. The radiance over a surface with albedo q is found by use of a well-known formula of Chandrasekhar[29]:

$$I(\mu_0, \mu, \varphi) = D(\mu_0, \mu, \varphi) + q \frac{E_0(\mu_0)T(\mu)}{1 - qc_0}. \quad \text{(A6)}$$

B. Delta-M Method

As the particle size increases, the scattered light is increasingly concentrated in a narrow peak in the forward-scattering direction. Accurate Legendre expansion of such functions requires thousands of terms. In these conditions, the convergence of a solution with an increasing order of MSH is slow, which explains why RT calculations for cloudy atmospheres have always been challenging.

To accelerate calculations, various approximations have been developed.[25] In the SHARM code we have implemented the Delta-M method,[13] which approximates the forward peak with a δ function:

$$\chi(\gamma) = F2\delta(0) + (1 - F)\chi^*(\gamma), \quad \text{(A7)}$$

where F is a fraction of forward scattering. The Delta-M method automatically conserves the first N moments of expansion:

$$\chi_n = F(2n + 1) + (1 - F)\chi_n^*, \quad \text{(A8)}$$

where

$$F = \frac{\chi_N}{2N + 1}, \qquad \chi_n^* = \frac{\chi_n - F(2n + 1)}{(1 - F)}.$$

The substitution of phase function (A7) into Eq. (A1a) leads to the modified problem

$$\mu \frac{\partial I}{\partial \tau^*} + I = \frac{\omega^*}{4\pi} \int_0^{2\pi} d\varphi' \int_{-1}^{1} \chi^*(\tau^*, \gamma) I(\tau^*, \mu', \varphi') d\mu' + S_\lambda \frac{\omega^*}{4} \frac{\chi(\tau, \gamma_0)}{1 - F} \exp\left[-\frac{\tau^*(1 - \omega F)^{-1}}{\mu_0} \right], \quad \text{(A9)}$$

with truncated phase function $\chi^*(\gamma)$, scaled optical thickness, and single-scattering albedo

$$\tau^* = \tau(1 - \omega F), \quad \omega^* = \omega \frac{(1 - F)}{(1 - \omega F)}. \quad \text{(A10)}$$

The new equation (A9) has the same form as the original one but with scaled parameters and a modified single-scattering source function.

Figure 1 shows the convergence of the SHARM code with and without the Delta-M method for calculations with the phase function of cirrus cloud. The accurate result corresponds to the converged high-order MSH solution ($nb = 512$). Except in the aureole region and in a transitional zone of $\sim 20°$, the low-order $nb = 32$–48 Delta-M solution has an accuracy within approximately 1–2%.

2. Surface BRF Models

Because there are different definitions of angles in the literature, and even differences in the formulation of BRF models are not unusual, we consider it worthwhile to give analytical expressions that are coded in SHARM. For convenience of notation, the cosine of the zenith angle below is always positive, and the upward view directions are indicated as $(-\mu)$.

A. Land: RPV and MRPV Models

The RPV model depends on three parameters (ρ_0, k, α):

$$\rho(\mu_0; -\mu; \varphi) = \rho_0 M(k) F(\alpha) H(\rho_0), \quad \text{(A11)}$$

$$M(k) = [\mu\mu_0(\mu + \mu_0)]^{k-1},$$

$$F(\alpha) = \frac{1 - \alpha^2}{[1 - 2\alpha \cos\gamma + \alpha^2]^{3/2}},$$

$$H(\rho_0) = \left(1 + \frac{1 - \rho_0}{1 + G}\right), \quad \text{(A12)}$$

where γ is the angle of scattering:

$$\cos\gamma = -\mu_0\mu + \sqrt{1 - \mu_0^2}\sqrt{1 - \mu^2}\cos(\varphi - \varphi_0), \quad \text{(A13)}$$

$$G = [\tan^2\theta_0 + \tan^2\theta + 2\tan\theta_0 \tan\theta \times \cos(\varphi - \varphi_0)]^{1/2}. \quad \text{(A14)}$$

Note that the hot spot lies in the direction of backscattering, $\varphi - \varphi_0 = \pi$.

Usually, Minnaert's exponent k is less than 1. This means that, at small values of μ and μ_0, the total BRF may become unphysically large and the surface albedo at high SZA may exceed 1. As a remedy, our algorithm sets the low limit of μ and μ_0 in BRF calculations to 0.03. This approach provides a stable solution for the common cases.

In the MRPV model, $F(\alpha)$ is replaced by $F(\alpha) = \exp(\alpha \times \cos\gamma)$. This modification yields a nearly linear expression for the BRF model parameters after logarithmic transformation.

B. Land: Linear LSRT Model

The linear LSRT model is represented by a sum of Lambertian, geometric-optics, and volume scattering terms:

$$\rho(\mu_0, -\mu, \varphi) = k_L + k_{go} f_{go}(\mu_0, \mu, \varphi) + k_v f_v(\mu_0, \mu, \varphi). \quad \text{(A15)}$$

The kernel functions are given by the following expressions:

$$f_v = \frac{(\pi/2 - \gamma)\cos\gamma + \sin\gamma}{\mu_0 + \mu} - \frac{\pi}{4}, \quad \text{(A16)}$$

$$f_{go} = O(\mu_0, \mu, \varphi) - \mu'^{-1} - \mu_0'^{-1} + \frac{1}{2}(1 + \cos\gamma')\mu'^{-1}\mu_0'^{-1}, \quad \text{(A17)}$$

where

$$O(\mu_0, \mu, \varphi) = \frac{1}{\pi}(t - \sin t \cos t)(|\mu'|^{-1} + \mu_0'^{-1}), \quad \text{(A18)}$$

$$\cos t = \frac{h}{b}\frac{\{(G')^2 + [\tan\theta_0' \tan\theta' \sin(\varphi - \varphi_0)]^2\}^{1/2}}{|\mu'|^{-1} + \mu_0'^{-1}}, \quad \text{(A19)}$$

with the constraint that $|\cos t| \le 1$. The primed angles (θ_0', θ') are obtained by scaling $\tan\theta' = (b/r)\tan\theta$. Note that $\cos\gamma'$ in Eq. (A17) and G' in Eq. (A19) are calculated for primed angles (θ'_0, θ') by use of Eqs. (A13) and (A14), respectively.

The ratio of structural parameters is fixed[20] ($h/b = 2$ and $b/r = 1$). Thus functions f_v and f_{go} depend on angles only, and the BRF is defined by three coefficients $\{k_L, k_{go}, k_v\}$.

It is important to keep in mind that functions f_v and f_{go} take both positive and negative values. Our experience with processing MISR measurements[30] shows that the best-fit weights k_{go} and k_v for different land-cover types are often negative, although the resultant BRF and surface albedo remain positive. For this reason, different terms of this model should be considered only as mathematical functions rather than physical components of the surface reflectance. Also, one needs to exercise caution with this model at zenith angles larger than 80°, when the BRF may become negative or, on the contrary, grow large.[31]

C. Ocean: Azimuthally Independent Model of Nakajima and Tanaka

Following Nakajima and Tanaka,[21] the reflection coefficient is expressed as follows:

$$R(\mu', -\mu, \varphi - \varphi') = \frac{1}{4\mu\mu_n} R^{Fr}(\chi) P(\mu_n) S(\mu', \mu), \quad \text{(A20)}$$

where R^{Fr} is the Fresnel reflectance for unpolarized radiance, $P(\mu_n)$ is the probability density function of the wave slope distribution, and S is the wave shadowing factor. The value of the refractive index of water that is required for computing R^{Fr} is obtained by spline interpolation from spectral data of Hale and Querry.[32]

The probability density function of the slope distribution is given by

$$P(\mu_n) = \frac{1}{\pi\sigma^2\mu_n^3}\exp\left(-\frac{1 - \mu_n^2}{\sigma^2\mu_n^2}\right), \quad \text{(A21)}$$

where $\sigma^2 = 0.00534u$, and u [m/s] is the wind speed 10 m above the water surface. Following Gordon and Wang,[33]

$$\frac{1}{4\mu\mu_n} P(\mu_n) = \frac{a^2}{\mu\pi\sigma^2}\exp\left(\frac{1 - 2a}{\sigma^2}\right),$$

where

$$a = \frac{1 + \cos 2\chi}{(\mu + \mu')^2},$$

$$\cos 2\chi = \mu\mu' - \sqrt{1 - \mu^2}\sqrt{1 - \mu'^2} \times \cos(\varphi - \varphi').$$

Finally, the wave-shadowing factor is written as

$$S(\mu', \mu) = \frac{1}{1 + F(g) + F(g')}, \quad g = \frac{\mu}{\sigma\sqrt{1 - \mu^2}},$$

where

$$F(g) = \frac{1}{2}\left[\frac{\exp(-g^2)}{g\sqrt{\pi}} - \frac{2}{\sqrt{\pi}}\int_g^\infty \exp(-t^2)dt\right] = \frac{\exp(-g^2)}{2g\sqrt{\pi}} - \frac{1}{2} + \Phi(\sqrt{2}g);$$

$$\Phi(\sqrt{2}g) = \frac{1}{\sqrt{2\pi}}\int_0^{\sqrt{2}g}\exp\left(-\frac{z^2}{2}\right)dz$$

is the probability integral for the normal distribution.

For compliance with the general form of the boundary condition [Eq. (A16)], the BRF is written as

$$\rho(\mu',\ -\mu,\ \varphi-\varphi') = \frac{\pi}{\mu'} R(\mu',\ -\mu,\ \varphi-\varphi').$$

D. Cox–Munk Model with the Gram–Charlier Expansion

Let us define the right-handed system of coordinates $(X,\ Y,\ Z)$ centered at observation point O. Vector OY lies in the principal plane and points in the direction opposite of the Sun, and vector OX is perpendicular to the principal plane. The wave slope (facet) has two components:

$$Z_x = \partial Z/\partial X = \sin\alpha \tan\beta = \frac{\sin\theta \sin\varphi}{\mu+\mu_0},$$

$$Z_y = \partial Z/\partial Y = \cos\alpha \tan\beta = \frac{\sin\theta\cos\varphi - \sin\theta_0}{\mu+\mu_0}, \quad \text{(A22)}$$

where α is the azimuth of ascent (clockwise from the Sun) and β is the tilt.

If the distribution of the slope components depends on the direction of the wind, let us rotate the coordinate system clockwise about axis OZ by angle $\Delta\varphi_w = \varphi_{\text{Wind}} - \varphi_0$. This yields a new coordinate system $(X',\ Y',\ Z')$, where axis OY' is aligned with the up-wind direction. In the new coordinates, slopes (A22) become

$$Z_u = Z_{y'} = Z_y \cos\Delta\varphi_w + Z_x \sin\Delta\varphi_w,$$

$$Z_c = Z_{x'} = -Z_y \sin\Delta\varphi_w + Z_x \cos\Delta\varphi_w. \quad \text{(A23)}$$

The slopes' probability density function can now be written as

$$P(\mu_n) = \frac{1}{2\pi\sigma_u\sigma_c{\mu_n}^3} \exp\left(-\frac{\xi^2+\eta^2}{2}\right)\text{GC},$$

$$\eta = Z_u/\sigma_u,\ \xi = Z_c/\sigma_c. \quad \text{(A24)}$$

The subscripts u and c refer to the up-wind and cross-wind components, and GC denotes the Gram–Charlier expansion.[22]

In the SHARM code the diffuse reflected radiance is always computed with the isotropic Nakajima–Tanaka model, and the directly reflected radiance can be computed with either that model or the Cox–Munk model. In the latter case the two models are linked by the energy conservation condition ${\sigma_U}^2 + {\sigma_C}^2 = {\sigma_{NT}}^2 = 0.00534u$. In their experiments, Cox and Munk observed a range of anisotropy $\sigma_u/\sigma_c = 1$–1.8, with an average value of 1.34. Currently the SHARM uses the values ${\sigma_U}^2 = 0.6\,{\sigma_{NT}}^2$ and ${\sigma_C}^2 = 0.4\,{\sigma_{NT}}^2$, so $\sigma_U/\sigma_C = 1.5$.

This research was supported by NASA Earth Observing System Science and NASA National Polar Orbiting Environmental Satellite System Preparatory Project grants.

References

1. M. D. King, W. P. Menzel, Y. J. Kaufman, D. Tanre, B. C. Gao, S. Platnick, S. A. Ackerman, L. A. Remer, R. Pincus, and P. A. Hubanks, "Cloud and aerosol properties, precipitable water, and profiles of temperature and humidity from MODIS," IEEE Trans. Geosci. Remote Sens. **41,** 442–458 (2003).
2. C. O. Justice, J. R. G. Townshend, E. F. Vermote, E. Masuoka, R. E. Wolfe, N. Saleous, D. P. Roy, and J. T. Morisette, "An overview of MODIS land data processing and product status," Remote Sens. Environ. **83,** 3–15 (2002).
3. D. J. Diner, J. C. Beckert, T. H. Reily, C. J. Bruegge, J. E. Conel, R. A. Kahn, J. V. Martonchik, T. P. Ackerman, R. Davies, S. A. W. Gerstl, H. R. Gordon, J.-P. Muller, R. B. Myneni, P. J. Sellers, B. Pinty, and M. M. Verstraete, "Multi-angle Imaging SpectroRadiometer (MISR) instrument description and experiment overview," IEEE Trans. Geosci. Remote Sens. **36,** 1072–1087 (1998).
4. B. N. Holben, T. F. Eck, I. Slutsker, D. Tanré, J. P. Buis, A. Setzer, E. Vermote, J. A. Reagan, Y. J. Kaufman, T. Nakajima, F. Lavenu, I. Jankowiak, and A. Smirnov, "AERONET—a federated instrument network and data archive for aerosol characterization," Remote Sens. Environ. **66,** 1–16 (1998).
5. K. Stamnes, S. C. Tsay, W. Wiscombe, and K. Jayaweera, "Numerically stable algorithm for discrete-ordinate-method radiative transfer in multiple scattering and emitting layered media," Appl. Opt. **27,** 2502– 2509 (1988).
6. E. F. Vermote, D. Tanre, J. L. Deuze, M. Herman, and J.-J. Mocrette, "Second Simulation of the Satellite Signal in the Solar Spectrum, 6S: an overview," IEEE Trans. Geosci. Remote Sens. **35,** 675–686 (1997).
7. K. F. Evans, "The spherical harmonics discrete ordinate method for three-dimensional atmospheric radiative transfer," J. Atmos. Sci. **55,** 429–446 (1998).
8. J. R. Key, "Streamer—User's guide" (University of Wisconsin, Madison, 2002); available at http://stratus.ssec.wisc.edu/streamer/streamer.html.
9. B. Mayer and A. Kylling, "Technical Note: The libRadtran software package for radiative transfer calculations: description and examples of use," Atmos. Chem. Phys. **5**. 1855–1877 (2005).
10. P. Ricchiazzi, S. Yang, C. Gautier, and D. Sowle, "SBDART: a research and teaching software tool for plane-parallel radiative transfer in the Earth's atmosphere," Bull. Am. Meteor. Soc. **79,** 2101–2114 (1998).
11. T. Z. Muldashev, A. I. Lyapustin, and U. M. Sultangazin, "Spherical harmonics method in the problem of radiative transfer in the atmosphere–surface system," J. Quant. Spectrosc. Radiat. Transfer **61,** 393–404 (1998).
12. A. I. Lyapustin and T. Z. Muldashev, "Generalization of Marshak boundary condition for non-Lambert reflection," J. Quant. Spectrosc. Radiat. Transfer **67,** 457–464 (2000).
13. W. J. Wiscombe, "Delta-M method—rapid yet accurate radiative flux calculations for strongly asymmetric phase functions," J. Atmos. Sci. **34,** 1408–1422 (1977).
14. W. Wiscombe, "Improved Mie scattering algorithms," Appl. Opt. **19,** 1505–1509 (1980).
15. A. Lyapustin, *SHARM Manual* (NASA GSFC, 2005); available at ftp://ltpftp.gsf.nasa.gov/projects/asrvn.
16. F. X. Kneizys, L. W. Abreu, G. P. Anderson, J. H. Chetwynd, E. P. Shettle, A. Berk, L. S. Bernstein, D. C. Robertson, P. Acharya, L. S. Rothman, J. E. A. Selby, W. O. Gallery, and

S. A. Clough, "The MODTRAN 2/3 report and LOWTRAN 7 model," (Ontar Corporation, North Andover, Mass., 1996).
17. B. A. Bodhaine, N. B. Wood, E. G. Dutton, and J. R. Slusser, "On Rayleigh optical depth calculations," J. Atmos. Ocean. Technol. **16,** 1854–1861 (1999).
18. H. Rahman, B. Pinty, and M. M. Verstraete, "Coupled surface-atmosphere reflectance (CSAR) model. 2. Semiempirical surface model usable with NOAA advanced very high resolution radiometer data," J. Geophys. Res. **98,** 20,791–20,801 (1993).
19. J. V. Martonchik, D. J. Diner, B. Pinty, M. M. Verstratete, R. B. Myneni, Yu. Knyazikhin, and H. R. Gordon, "Determination of land and ocean reflective, radiative and biophysical properties using multiangle imaging," IEEE Trans. Geosci. Remote Sens. **36,** 1266–1281 (1998).
20. W. Lucht, C. B. Schaaf, and A. H. Strahler, "An algorithm for the retrieval of albedo from space using semiempirical BRDF models," IEEE Trans. Geosci. Remote Sens. **38,** 977–998 (2000).
21. T. Nakajima and M. Tanaka, "Effect of wind-generated waves on the transfer of solar radiation in the atmosphere–ocean system," J. Quant. Spectrosc. Radiat. Transfer **29,** 521–537 (1983).
22. C. Cox and W. Munk, "Measurements of the roughness of the sea surface from photographs of the Sun's glitter," J. Opt. Soc. Am. **44,** 838–850 (1954).
23. A. Lyapustin, "Radiative transfer code SHARM-3D for radiance simulations over a non-Lambertian nonhomogeneous surface: intercomparison study," Appl. Opt. **41,** 5607–5615 (2002).
24. C. K. Gatebe, M. D. King, A. I. Lyapustin, G. T. Arnold, and J. Redemann, "Airborne spectral measurements of ocean directional reflectance," J. Atmos. Sci. **62,** 1072–1092 (2005).
25. T. Nakajima and M. Tanaka, "Algorithm for radiative intensity calculations in moderately thick atmospheres using a truncation approximation," J. Quant. Spectrosc. Radiat. Transfer **40,** 51–69 (1988).
26. A. Lyapustin, "Interpolation and profile correction (IPC) method for shortwave radiative transfer in spectral intervals of gaseous absorption," J. Atmos. Sci. **60,** 865–871 (2003).
27. A. H. Karp, J. Greenstadt, and J. A. Fillmore, "Radiative transfer through an arbitriarily thick, scattering atmosphere," J. Quant. Spectrosc. Radiat. Transfer **24,** 391–406 (1980).
28. J. V. Dave, "A direct solution of the spherical harmonics approximation to the radiative transfer equation for an arbitriary solar elevation," J. Atmos. Sci. **32,** 790–798 (1975).
29. S. Chandrasekhar, *Radiative Transfer* (Dover, 1960).
30. A. Lyapustin, Y. Wang, J. Martonchik, J. Privette, B. Holben, I. Slutsker, A. Sinyuk, and A. Smirnov, "Local analysis of MISR surface BRF and albedo over GSFC and Mongu AERONET sites," IEEE Trans. Geosci. Remote Sens. (to be published).
31. F. Gao, X. Li, A. Strahler, and C. Schaaf, "Evaluation of the Li transit kernel for BRF modeling," Remote Sens. Rev. **19,** 205–224 (2000).
32. G. M. Hale and M. R. Querry, "Optical constants of water in the 200-nm to 200-μm wavelength region," Appl. Opt. **12,** 555–563 (1973).
33. H. R. Gordon and M. Wang, "Surface-roughness considerations for atmospheric correction of ocean color sensors. I. The Rayleigh-scattering component," Appl. Opt. **31,** 4247–4260 (1992).